ORAL REFERNCE: *0554*

PLASTIC-DAMAGE MODEL FOR STRESS-STRAIN BEHAVIOR OF SOILS

N. A. Al-Shayea[1], K. R. Mohib[1], and M. H. Baluch[1]

[1] Department of Civil Engineering, KFUPM, Dhahran 31261, Saudi Arabia

ABSTRACT

This paper presents a constitutive model for soil, which combines plasticity with damage mechanics to simulate the stress-strain behavior. This model is primarily suitable for soil types that exhibit a post-peak strain-softening behavior, like dense sand and stiff clay. The post-peak stress drop is captured by the elasto-damage formulation, while the plasticity is superimposed beyond the elastic range. The total strain increment is composed of elasto-damage strain increment and plastic strain increment. The elasto-damage strain increment is found using the elasto-damage formulation, while the plastic strain increment is found as a function of damage strain. To calibrate this model, Triaxial tests were conducted on cohesive and cohesionless soils, to obtain the model parameters. The model was coded in computer programs to simulate the stress-strain behavior of soils. The model was verified and found to predict the response of geomaterials well.

Key words: Damage mechanics, soil plasticity, strain softening, confining pressure.

INTRODUCTION

A plasto-damage model was developed for stress-strain behavior of cohesive and non-cohesive soils. The model was customized for the case of conventional triaxial compression (CTC), because of the abundant use of this test for determination of soil strength. Dense soils investigated in this work have damage effect, which is the degradation in material compliance, along with the plasticity effect, which is the irrecoverable permanent deformation. The elasto-damage component of the strain was obtained from the elasto-damage formulation derived for the CTC test. The post-peak stress-drop was also picked by the damage formulation. The plastic strain was taken as some factor times the damage strain. The total strain increment ($d\varepsilon$) is composed of elastic increment ($d\varepsilon^e$), damage increment ($d\varepsilon^d$), and plastic increment ($d\varepsilon^p$); i.e., $d\varepsilon = d\varepsilon^e + d\varepsilon^d + d\varepsilon^p$.

Analytical formulation was carried out to obtain the plasto-damage stress-strain behavior. Also, experimental program was conducted on two different types of soil to find model parameters. Furthermore, computer programs were developed based on the analytical formulation to simulate the soil behavior.

LITERATURE REVIEW

The theory of continuum damage mechanics (CDM) proposed by Kachanov [1], has been applied successfully to different materials, and is used to predict both strain-hardening and strain-softening type of behaviors. The damage phenomenon is explained in terms of damage variable (ω_n) associated with the normal $\vec{n}$, represents the area of the cracks and cavities per unit surface in a plane perpendicular to $\vec{n}$. Therefore, $\omega_n = 0$ corresponds to the undamaged state, $\omega_n = 1$ corresponds to the rupture of the element in two parts; and $0 < \omega_n < 1$ characterizes the occurrence of damage.

Chow [2] presented a modified damage effect tensor $\widetilde{M}(D)$ for the effective stress equations to take into account the effect of anisotropic material damage. Their model was applied on metals. Chow [3] developed a generalized damage characteristic tensor ($\widetilde{J}$), to characterize anisotropic damage evolution in combination with plasticity.

Sauris [4] presented a damage model for monotonic and cyclic loading of concrete. The compliance tensor presented for stress strain relationship was dependent on accumulated damage. Damage evolution was obtained by using a loading surface (f), a bounding surface (F), and a limit fracture surface (f_o); all defined in terms of the thermodynamic force conjugates of the damage variables. The model was applied for the case where the principal stresses and the strain axes coincided and did not rotate as the material deformed.

Abu-Labdeh [5] presented plasticity damage model for concrete under cyclic multi-axial loading. The model was based on bounding surface concept and combined plastic deformations with deformations due to damage. The total strain increment ($d\varepsilon$) was divided into elastic strain increment ($d\varepsilon^e$), damage strain increment ($d\varepsilon^d$) and plastic strain increment ($d\varepsilon^p$). Crouch [6] presented a constitutive model, which treated clays, silts, and sand in their loose and dense state under both monotonic and complex stress paths.

Karr [7] presented brittle damage model for rock. In their model, the effect of material degradation on failure mechanism of brittle damage materials was investigated. Gupta [8] presented a model for compressive failure of rocks via process of shear faulting. The model presented the progressive growth of damage. Khan [9] proposed a constitutive model for concrete based on CDM, using the damage-effect tensor ($\widetilde{M}$) with damage magnification factor α and β for tension and compression, respectively. The bounding surface concept, as introduced by Dafalias [10], was used for the constitutive relationship and evolution of damage.

DAMAGE FORMULATION FOR CTC

For the case of CTC test, $\sigma_2 = \sigma_3 = \sigma_{cell}$ = constant, and the deviator stress in the axial direction ($\Delta\sigma_1$) is changing. This case reduces to a uniaxial case. The deviator part of the of the stress vector, causing the shearing failure in the cylindrical soil specimen, is given as:

$$\sigma_{deviator} = \begin{bmatrix} \Delta\sigma_1 & 0 & 0 \end{bmatrix}^T \tag{1}$$

For CTC test, the compliance and stiffness terms for i = j = 1, with $\omega_1 = 0$ and $\omega_2 = \omega_3 = \omega$, are:

$$\widetilde{C}_{11} = \frac{1}{E_o(1-\beta\omega)^4}, \quad \text{or} \qquad \widetilde{D}_{11} = E_o(1-\beta\omega)^4 \tag{2}$$

where, E_o is the initial modulus of elasticity, and β is the peak strength factor or damage magnification factor. The strain energy density (ρW) for the deviator part of the CTC test is:

$$\rho W = \frac{1}{2}\{\sigma_i\}^T\left[\widetilde{C}_{ij}\right]\{\sigma_j\} = \frac{1}{2}\Delta\sigma_1^2\widetilde{C}_{11}^2 = \frac{1}{2}\frac{\Delta\sigma_1^2}{E_o}\left[\frac{(1-\beta\omega_1)^2}{(1-\beta\omega_2)^2(1-\beta\omega_3)^2}\right] \tag{3}$$

where, $\widetilde{C}_{ij}$ = effective compliance matrix, inverse of the effective stiffness matrix $\widetilde{D}_{ij}$, and

$\Delta\sigma_1$ = $\varepsilon_1 E_o \dfrac{(1-\beta\omega_2)^2(1-\beta\omega_3)^2}{(1-\beta\omega_2)^2}$

The thermodynamic force conjugates (R_i) can be obtained by taking the negative derivative of (ρW) with respect to (ω_n), which gives $R_1 = 0$ and $R_2 = R_3 = \varepsilon_1^2 E_o \beta(1-\beta\omega)^3$. R_1 is set to zero because a negative value of a thermodynamic force conjugate makes no physical sense and is not compatible with the thermodynamic conditions. This means that damage in this direction is also zero, i.e., $\omega_1 = 0$. For the CTC test, $\omega_2 = \omega_3 = \omega$, due to symmetry. The expression for strain energy release rate at onset of damage (R_o) is given as a function of $\Delta\sigma$, which is some percentage of the peak deviator strength ($\Delta\sigma_1$), according to:

$$R_o = \frac{\sqrt{2}\beta\Delta\sigma^2}{E_o} \tag{4}$$

The expression for critical value of strain energy release rate at failure (R_c) is given as:

$$R_c = \frac{\sqrt{2}\beta\Delta\sigma_1^2}{E_o(1-\beta\omega)^5} \tag{5}$$

For the deviatoric stress increment in axial direction is:

$$d\sigma_1 = \widetilde{D}_{11}d\varepsilon_1 - \varepsilon_1\frac{\partial\widetilde{D}_{11}}{\partial\omega_k}\frac{\partial f}{\partial R_k}d\lambda \tag{6}$$

where, $d\lambda$ = $\dfrac{2\sqrt{2}\beta\varepsilon_1 E_o(1-\beta\omega)^3 d\varepsilon_1}{\left(H + 3\beta^2\varepsilon_1^2 E_o(1-\beta\omega)^2\right)}$,

H = $D\delta/\langle\delta_{in}-\delta\rangle$ = damage modulus,

δ = normalized distance between f and F surfaces,

δ_{in} = maximum distance between F and f_o surfaces, and

D = parameter used to control the shape of the peak.

Substituting all the terms in Eqn. 6, the final form of the incremental stress for a strain-controlled formulation becomes:

$$d\sigma_1 = \left[E_o(1-\beta\omega)^4 - \frac{8\beta^2\varepsilon_1^2 E_o^2(1-\beta\omega)^6}{H + 3\beta^2\varepsilon_1^2 E_o(1-\beta\omega)^2}\right]d\varepsilon_1 \tag{7}$$

For the determination of the elasto-damage stress, Eqn. 7 was coded in a FORTRAN program, with inputs including the axial elasto-damage strain increment.

EXPERIMENTAL PROGRAM

In order to calibrate the model and to determine its parameters, an extensive experimental program was conducted. Two different types of soil materials were used, i.e., cohesive and non-cohesive soil (marl and sand). Both soils were prepared at high density to exhibit post-peak strain-softening behavior. Marl was tested at maximum value of dry density of 1.526 g/cm^3 and at optimum moisture content of 27.12% obtained form the compaction test. The minimum and maximum densities of sand were 1.86 g/cm^3 and 1.609 g/cm^3, respectively. Marl samples were prepared at the maximum density and optimum moisture content using in five layers under static compaction, to get uniform sample. Sand was tested at a density of 1.853 g/cm^3, which corresponds to a relative density of 98%. Pluviation technique was used for preparing sand samples. Unconsolidated drained triaxial compression tests were performed at cell pressures of 100, 200, 300, 400, and 500 KPa, for both soils. Testing apparatus were calibrated to ensure accurate measurements of stresses and strains.

RESULTS AND DISCUSSIONS

Elasto-damage parameters

Mechanical properties

The shear strength parameters, cohesion (c) and angle of internal friction (ϕ), were determined using the peak deviator stress value ($\Delta\sigma_1$) at different cell pressure values, by plotting Mohr stress circles and Mohr-Coulomb failure envelopes for both soils. For marl $\phi = 33.73°$ and c = 335 KPa. For sand $\phi = 42.96$ ° and $c = 0$. The initial modulus of elasticity (E_o) was obtained as the slope of the initial straight-line portion of the experimental stress-strain curve, for various values of cell pressure (σ_3). Expressions for E_o vs. σ_3 normalized to atmospheric pressure (P_a=101.325 KPa) are:

$$E_o = 682.5 P_a \left(\sigma_3 / P_a\right)^{0.238156} \quad \text{, for marl} \tag{8}$$

$$E_o = 1176.06 P_a \left(\sigma_3 / P_a\right)^{0.862364} \text{, for sand} \tag{9}$$

Strain Energy release rates

R_o was calculated using Eqn. 4 at 20% and 30% of the peak deviator stress value for marl and sand, respectively. This was decided on the basis of the experimental stress-strain data. The values of R_c were calculated using Eqn. 5, and found to be 0.1 and 0.2 KN.m/m^3 for marl and sand, respectively. These are the minimum values of R_c calculated at different cell pressures.

Peak factors (D) and (β)

The value of the peak shape factor (D) for marl and sand was found by trial and error, to be 0.0001 KN.m/m^3. The value of peak deviator stress factor (β) was calculated by matching the peak of the predicted stress-strain curve with the experimental curve. Figure 1-a shows the variation of β vs. peak deviator stress ($\Delta\sigma_1$) for marl and sand, which can be expressed as:

$$\beta = 0.5697 / \left(\Delta\sigma_1\right)^{0.916701} \quad \text{, for marl} \tag{10}$$

$$\beta = 0.87782 / \left(\Delta\sigma_1\right)^{0.785059} \quad \text{, for sand} \tag{11}$$

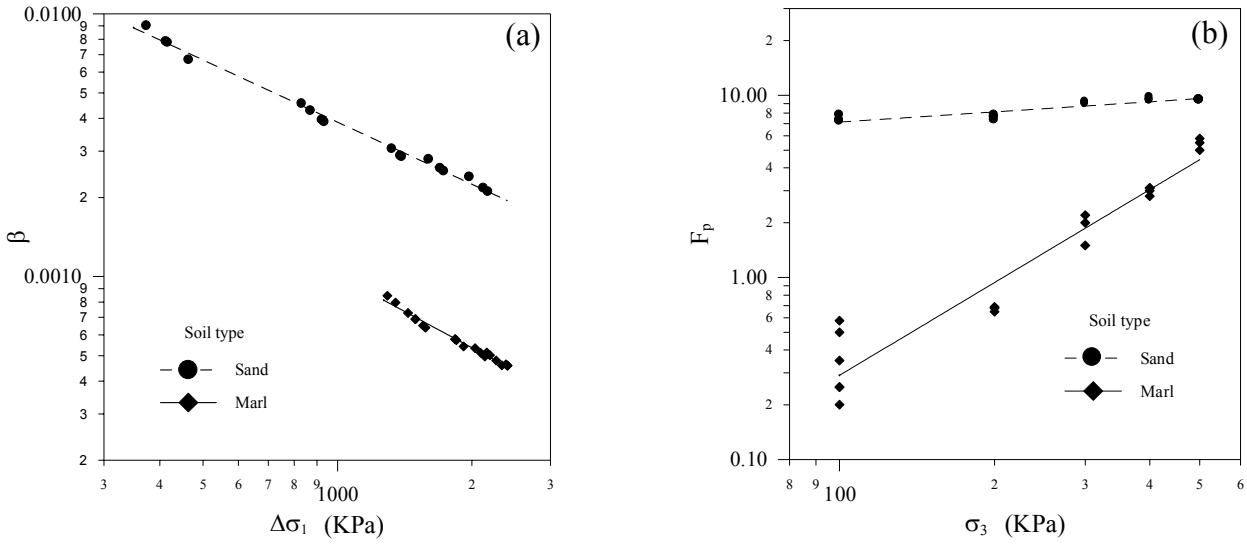

Figure 1: Model parameters: (a) β vs. $\Delta\sigma_1$, and (b) F_p vs. σ_3

Plastic strain

Plastic strain increment ($d\varepsilon^p$) was calculated as a factor (F_p) times the damage strain ($d\varepsilon^d$). Figure 1-b shows the variation of the plastic strain factor (F_p) with cell pressure (σ_3) for marl and sand, with the expressions:

$$F_p = 1.187 \times 10^{-4} (\sigma_3)^{1.694} \quad \text{, for marl} \tag{12}$$

$$F_p = 3.055 \times (\sigma_3)^{0.1845} \quad \text{, for sand} \tag{13}$$

The total strain was obtained by adding the plastic strain to the elasto-damage strain. Figure 2-a shows a comparison between the experimental and predicted stress-strain curve for sand at σ_3 = 200 KPa. It is clear that without the plastic strain component, the two curves are far apart from each other on the strain axis. After adding the plastic strain, the elasto-plasto-damage prediction, matches the experimental curve very closely. Figure 2-b shows a comparison between the experimental and the predicted stress-strain curves by this model at different cell pressures for sand. Similar curves were obtained for marl.

CONCLUSIONS

A new plasto-damage model is presented for the stress-strain behavior of dense soils. The model is suitable for post-peak strain-softening stress-strain behavior of soil. The model combines elasto- damage strain and plastic strain to determine the total strain. The predictions are excellent and able to pick all the features of the stress-strain behavior. It is observed that the model is good for both cohesive and non-cohesive types of soils. This model is very simple and needs few numbers of parameters to be calibrated. Only conventional triaxial test data is required, with no additional experimental data required for the calculation of plastic strain.

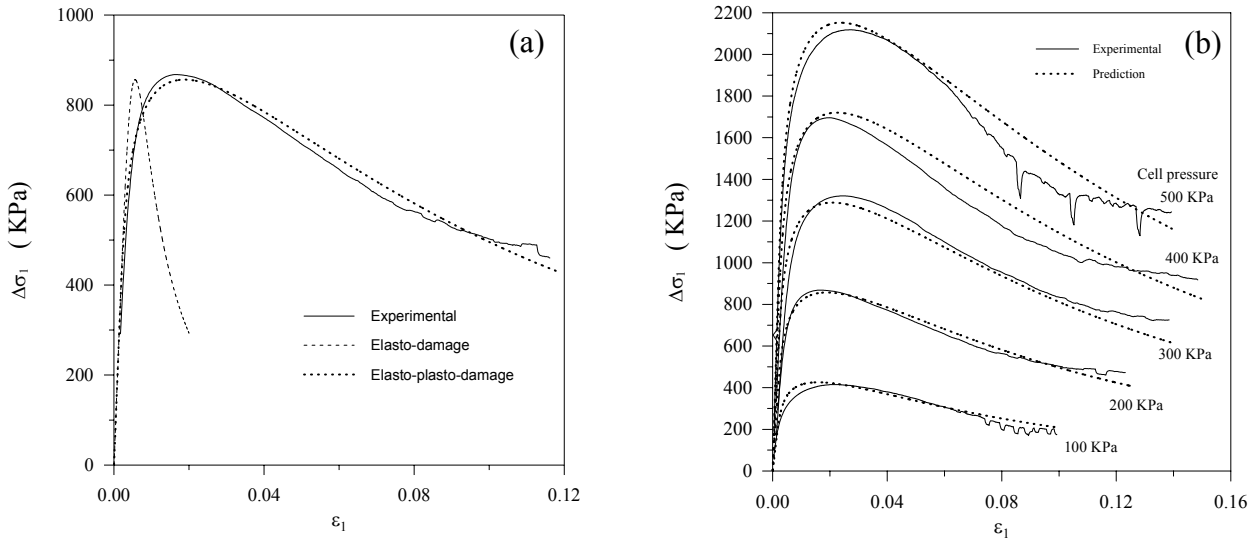

Figure 2: Comparison of stress-strain curves (a) Effect of Plastic strain, (b) curves for sand

ACKNOWLEDGEMENT

The authors acknowledge the support of King Fahd University of Petroleum and Minerals for providing computing and laboratory facilities. The help of Dr. Asad-ur-Rehman Khan is greatly appreciated.

REFERENCES

1. Kachanov, L. M. (1958). *Time of the Rupture Process under Creep condition*: Izv Akad Nauk, U.S.S.R, Otd. Tekh. Nauk,Vol. 8, pp. 26-31.
2. Chow, C.L. and Wang, J. (1987). *An Anisotropic Theory of Elasticity for Continuum Damage Mechanics: International Journal of Fracture*, pp. 3-16.
3. Chow, C. L. and Wang, J. (1988). *A finite Element Analysis of Continuum Damage Mechanics for Ductile Fracture: Engineering Fracture Mechanics*, pp. 83-102.
4. Sauris, W., Ouyang, C., and Ferdenando, V. M. (1990). *Damage Model for Cyclic Loading of Concrete: Journal of Engineering Mechanics and Physics*, pp. 1020-1035.
5. Abu-Lebdeh, T. M. and Voyiadjis, G. Z. (1993). *Plasticity Damage Model for Concrete under Cyclic Multi-axial Loading: Journal of Engineering Mechanics*, pp. 1465-1484.
6. Crouch, R. S. and Wolf J. P., (1995). *On a Three-Dimensional Anisotropic Plasticity Model for Soil: Geotechnique*, 45(2), pp. 301-305.
7. Karr, D. G., Wimmer, S. A., and Sun, X. (1996). *Shear Band Initiation of Brittle Damage Materials: International Journal of Damage Mechanics*, Vol. 5, pp. 403-421.
8. Gupta, V., and Bergstrom, J. S. (1997). *Compressive Failure of Rocks: International Journal of Rock mechanics and Mining Science*, Vol. 34, No.3-4.
9. Khan, A. R., Al-Gadhib, A. H. and Baluch, M. H. (1998). *An Elasto Damage Constitutive Model for High Strength Concrete: Proceedings of the Euro-C 1998 Conference on Computational Modeling of Concrete Structures*, Austria, pp. 133-142.
10. Dafalias, Y. F., and Popov, E. P. (1977). *Cyclic Loading for Material with a Vanishing Elastic Region: Nuclear Engineering Design*, Vol. 44, pp. 293-302.